Available online at www.sciencedirect.com
SCIENCE DIRECT®
Building and Environment 41 (2006) 699–709
BUILDING AND ENVIRONMENT
www.elsevier.com/locate/buildenv

Effect of reference state on the performance of energy and exergy evaluation of geothermal district heating systems: Balcova example

Leyla Ozgener[a,*], Arif Hepbasli[b], Ibrahim Dincer[c]

[a]Graduate School of Natural and Applied Sciences, Mechanical Engineering Science Branch, Ege University, 35100 Bornova, Izmir, Turkey
[b]Department of Mechanical Engineering, Faculty of Engineering, Ege University, 35100 Bornova, Izmir, Turkey
[c]Faculty of Engineering and Applied Science, University of Ontario Institute of Technology (UOIT), 2000 Simcoe Street, North Oshawa Ont., Canada L1H 7K4

Received 28 January 2005; received in revised form 8 March 2005

Abstract

In this paper, we undertake a parametric study to investigate how varying reference temperature from 0 to 25 °C will affect the energy and exergy efficiencies of the Balcova geothermal district heating system (BGDHS) and develop two significant correlations (with a correlation coefficient of 0.99) that can be used for predicting the efficiencies. The exergy losses in the overall BGDHS are quantified and illustrated using exergy flow diagram particularly for a reference temperature of 11.4 °C for comparison purposes. This reference temperature is taken as an average value of the ambient temperatures measured during the past 5 years for the day of 2nd January to reflect the actual situation. The results show that the exergy losses within the system occur mainly due to the losses in pumps, heat exchangers, reinjection sections of the geothermal water back into reservoir and pipeline, and account for 1.75%, 8.84%, 14.20%, and 28.69%, respectively. In addition, we study energy and exergy efficiencies to determine the possibilities to improve the system, and energy and exergy efficiencies of the system are found to be 42.36% and 46.55%, respectively, for 2nd January 2004.

Keywords: Geothermal energy; Energy; Exergy; Efficiency; Renewable energy

1. Introduction

Geothermal energy appears to be a potential solution to energy and environmental problems, where it is available, and a key tool for betterment of society and its sustainable future. The other advantage is that geothermal energy systems are simple, safe and adaptable (with modular up to about 50 MW). Due to their advantages, they are given priority in both developed and developing countries as an attractive option to replace fossil fuels [1].

Some energy and exergy values are dependent on the intensive properties of the reference state. Consequently, the results of energy and exergy analyses generally are sensitive to variations in these properties. Before energy and exergy analyses can be applied with confidence to energy systems, e.g., geothermal district heating systems, the significance of the sensitivities of energy- and exergy-analysis results in reasonable variations in dead-state properties must be assessed. Only very brief discussions of these sensitivities have been reported (e.g., [2–4]). The authors believe that one requirement for continued acceptance of exergy analysis is that the effects on the results of exergy analyses of variations in dead-state properties be fully examined and understood.

Based on the studies on the energetic and exergetic aspects of geothermal systems appeared in the open

*Corresponding author. Tel.: +90 232 388 40 00x1242; fax: +90 232 388 60 27.
E-mail addresses: leylaozgener@mail.ege.edu.tr, ozgener@egenet.com.tr (L. Ozgener).

0360-1323/$ - see front matter © 2005 Elsevier Ltd. All rights reserved.
doi:10.1016/j.buildenv.2005.03.007

Nomenclature

$\dot{E}$	energy rate (kW)
EPLL	rate of energy loss due to water leaks in the distribution network (kW)
ETR	rate of energy loss due to thermal reinjection (kW)
$\dot{E}x$	exergy rate (kW)
ExHEL	rate of exergy destructions in the heat exchangers (kW)
ExPLL	rate of exergy loss due to water leaks in the distribution network (kW)
ExPu	rate of exergy destructions in the pumps (kW)
ExTR	rate of exergy loss due to thermal reinjection (kW)
h	specific enthalpy (kJ/kg)
$\dot{m}$	mass flow rate (kg/s)
n	number of wellhead (dimensionless)
$\dot{P}$	exergy rate of the product (kW)
P	pressure (kPa)
s	specific entropy (kJ/kg K)
$\dot{S}$	entropy rate (kW/K)
$\dot{W}$	power (kW)
T	temperature (K)
t	temperature (°C)
ExP	rate of exergy product (kW)
HEx	utilized power by heat exchanger (kW)
SExI	specific exergy index (dimensionless)
TEI	rate of total energy input (kW)
TExI	rate of total exergy input (kW)

Greek letters

η	energy efficiency (%)
ε	exergy efficiency (%)
ψ	specific exergy (kJ/kg)

Subscripts

a	ambient
c1	energy efficiency correlation
c2	exergy efficiency correlation
dest	destroyed
gen	generation
HE	heat exchanger
i	number of terms in series
in	inlet
k	item number
out	outlet
r	re-injected thermal water
t	thermal
Tot	total
0	reference state

Abbreviations

BGDHS	Balcova geothermal district heating system
W	water
TW	thermal water
TWR	thermal water re-injection

literature, we can classify them in three groups as follows: (i) exergy analysis of geothermal power plants [5–9] (ii) evaluation of geothermal fields using exergy analysis [10–12], and (iii) classification of geothermal resources by exergy [12]. The concept of exergy was first used to analyze a geothermal power plant by Badvarsson and Eggers [5]. Their illustrative example compared the performances of single and double flash cycles based on a reservoir water temperature of 250 °C and a sink condition of 40 °C with the exergy efficiencies of 38.7% and 49%, respectively [12]. In addition, numerous studies have been undertaken from fundamental studies to energy and exergy analyses of geothermal and thermal systems in general [4–14] and more recently, Ozgener et al. [14–16] and Ozgener [17] have conducted an exergy analysis of two local geothermal district heating systems in Turkey.

To the best of the authors' knowledge, no examination of the effects of the reference state on the efficiencies of the geothermal district heating systems has appeared in the literature. This was the motivation behind the present work. The authors undertook a preliminary study [16] on energy and exergy analyses of the Balcova geothermal district heating system at a reference temperature of 13.1 °C only. Here, we now present an original and more practical version of the energy and exergy analysis of the system at a more realistic reference temperature of 11.4 °C as the actual average local temperature, rather than the standard environment temperature and investigate the energy and exergy losses in the system at this particular practical temperature. Furthermore, we study the effects of varying reference state temperature from 0 to 25 °C on the energy and exergy efficiencies of the system and develop some practical correlations that are capable of predicting efficiencies at various ambient temperatures.

2. Case study

Fig. 1 illustrates a schematic diagram of the Balcova geothermal district heating system in Izmir, Turkey, including hotels and official buildings as heated by the system. It is situated on a total area of about 3.5 km^2

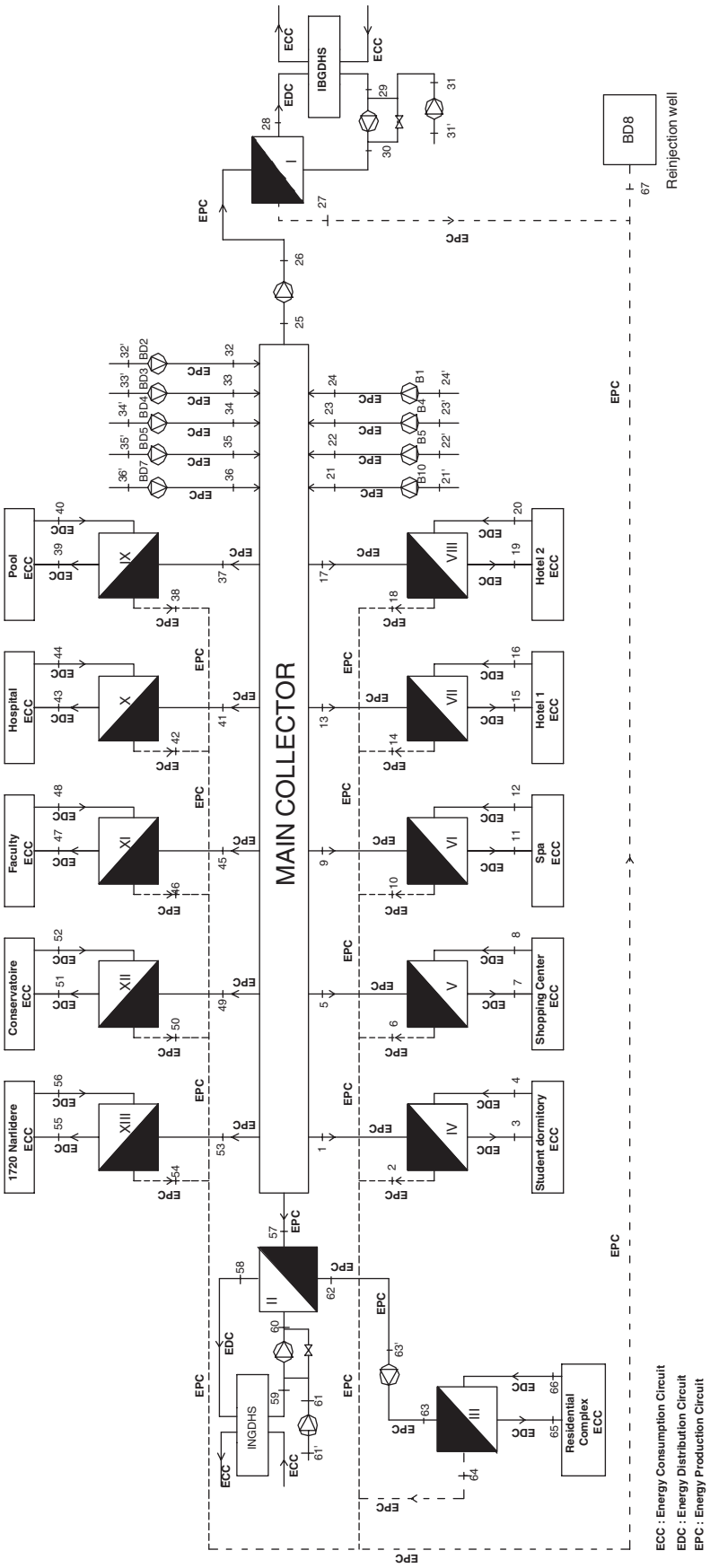

Fig. 1. Schematic layout of the BGDHS [16].

with an average thickness of the aquifer horizon of 150 m. There is no feeding, and only 25% of the fluid contained in the reservoir is utilized. A maximum yield of the field is about 205 kg/s at a reservoir temperature of 118 °C. The BGDHS consists mainly of three circuits, e.g., (a) EPC: energy production circuit (geothermal well loop—BDs, Bs, and BD8 reinjection wells lines); (b) EDC: energy distribution circuit (district heating distribution network—from main collector to heat exchangers (I–XIII) lines), and (c) ECC: energy consumption circuit partly described (building substations—from heat exchangers (I–XIII) to users' heat exchangers). Here, BDs stand for deep wells and Bs stand for shallow wells. At the end of 2001, there were 14 wells ranging in depth from 48 to 1100 m in the IBGF, while 10 wells were working at the date studied. Of these, eight wells (designated as BD2, BD3, BD4, BD5, BD7, B1, B4, B5, and B10) and one well (BD8) are production and reinjection wells, respectively. The temperatures of the production wells essentially vary from 95 to 140 °C, while the mass flow rates of the wells range from 8.3 to 41.7 kg/s, respectively. The thermal water is then sent to two primary plate-type heat exchangers and is cooled to about 60–62 °C [14], to heat the secondary fluid. The heat loss to surroundings is neglected everywhere (perfect insulation is assumed). The pressure drops due to the liquid flow friction in the study are also neglected.

The primary thermal water is reinjected into the well BD8 while the secondary fluid is utilized to heat the buildings through the substation heat exchangers. The average conversion temperatures obtained during the operation of the BGDHS are 80/57 °C for the district heating distribution network and 60/45 °C for the building circuit. Using the control valves for flow rate and temperature at the building substations the required amount of water is sent to each housing unit to achieve the heat balance of the system. The thermal water collected from the eight production wells at an average well heat temperature of 117.9 °C is pumped to a main collector (from eight production wells) with a total mass flow rate of about 212.16 kg/s.

Note that the ability to provide a continuous and adequate flow rate of high-temperature water from one or more production wells is a basic requirement for any geothermal heating scheme. The requirements of long-term reservoir management and environmental regulations which cover the treatment of waste geothermal fluids (thermal waters) may result in the use of one or more re-injection wells for disposal of wastewater from the scheme. The characteristics of the geothermal reservoir and particular features of the heating scheme will determine whether adequate flow rates can be maintained in both production and re-injection wells either by natural means or with the assistance of well pumps [18].

In the present case study on the BGDHS, the hourly recorded experimental thermal data of various parameters (e.g., temperatures, pressure and volumetric flow rates) were taken directly from the system technical staff who conducted the measurements of pressures and temperatures of fluids (including water and geothermal) through the Bourdon-tube pressure gauges and fluid-expansion thermometers, respectively. The volumetric flow rates of the distribution networks were measured by Danfoss MAG 3000 flowmeters. Then, we conducted an uncertainty/error analysis of the measurements and their derivatives using the Holman's uncertainty analysis technique as described in detail in [19]. As a result of this analysis, further information on technical details of the system and the total uncertainties of these measured and calculated parameters are given elsewhere [16].

The reference-state temperature value of 11.4 °C was obtained from the average ambient temperature data measured between 2000 and 2004 for 2nd January in Izmir. In this study, the reference state was considered varying from 0 to 25 °C and the state of environment at which the temperature and the atmospheric pressure are 11.4 °C and 101.32 kPa, respectively, which were the values measured at the time when the geothermal district heating system data were obtained.

3. Modeling

Here, Table 1 shows the general mass, energy and exergy balance equations to find the energy and exergy inputs and outputs, the rate of exergy decrease, the rate of irreversibility, and the energy and exergy efficiencies.

The balance equations are written for mass, energy and exergy flows in the system and its components as they are considered steady-state steady-flow control volume systems, and the appropriate energy and exergy equations are derived for this system and its components. The heat loss to the surroundings everywhere is neglected (a perfect insulation is assumed). The pressure drops due to the liquid flow friction in the study are also neglected.

In general, the mass balance equation can be expressed in the rate form as given in Eqs. (1) and (2) where $\dot{m}$ is the mass flow rate, and the subscript in stands for inlet and out for outlet.

The general energy balance equation for the steady-state steady-flow process is given in Eq. (3) in Table 1, where the total energy input is equal to total energy output. The reference-state temperature value of 11.4 °C was obtained from the average ambient temperature data measured between 2000 and 2004 for 2nd January in Izmir.

From all possible exergy components only the physical component of exergy is considered. The values for the total energy and exergy inputs to the BGDHS

Table 1
The general balance equations for the system and its components, along with efficiency equations

Equations	Eq. no.	Remarks
$\sum \dot{m}_{in} = \sum \dot{m}_{out}$	(1)	The general mass balance equation
$\sum_{l=1}^{n} \dot{m}_{TW,i,Tot} - \dot{m}_r - \dot{m}_d = 0$	(2)	Overall geothermal system mass balance equation
$\dot{E}_{in,i} = \dot{E}_{out,i}$	(3)	The general energy balance can be expressed as the total energy input equal to total energy output
$\dot{E}_{brine} = \dot{m}_{TW}(h_{brine} - h_0) = \sum_{i=21}^{n=24} \dot{m}_{TW,i}(h_i - h_0) + \sum_{i=32}^{n=36} \dot{m}_{TW,i}(h_i - h_0)$	(4)	Energy rate of thermal water (brine) (state number of brine: 21–24, 32–36)
$\psi = (h - h_0) - T_0(s - s_0)$	(5)	General specific exergy
$\dot{E}x_{brine} = \dot{m}_{TW}[(h_{brine} - h_0) - T_0(s_{brine} - s_0)] = \sum_{i=21}^{n=24} \dot{m}_{TW,i}[(h_i - h_0) - T_0(s_i - s_0)] + \sum_{i=32}^{n=36} \dot{m}_{TW,i}[(h_i - h_0) - T_0(s_i - s_0)]$	(6)	Exergy rate of thermal water (brine)
$\dot{E}x_{heat} - \dot{E}x_{work} + \dot{E}x_{mass,in} - \dot{E}x_{mass,out} = \dot{E}x_{dest}$	(7)	General exergy destruction in thermal systems
$\dot{E}x_{dest,pump} = \dot{W}_{pump} - (\dot{E}x_{out} - \dot{E}_{in})$	(8)	Exergy destruction in pump
$\dot{E}x_{dest,HE} = \dot{E}x_{in} - \dot{E}x_{out}$	(9)	Exergy destruction in heat exchanger
$\dot{E}x_{dest,system} = \sum \dot{E}x_{dest,HE} + \sum \dot{E}x_{dest,pump}$	(10)	Exergy destruction in the BGDHS
$\eta_{system} = \frac{\sum_{i=1}^{n=XIII} \dot{E}_{useful,HE,i}}{\dot{E}_{brine}}$	(11)	Energy efficiency of the BGDHS
$\varepsilon = \frac{\dot{E}x_{output}}{\dot{E}x_{input}}$	(12)	General exergy efficiency of BGDHS
$\varepsilon_{HE} = \frac{\dot{m}_{cold}(\psi_{cold,out} - \psi_{cold,in})}{\dot{m}_{hot}(\psi_{hot,in} - \psi_{hot,out})}$	(13)	Exergy efficiency of heat exchanger
$\varepsilon_{pump} = \frac{\dot{E}x_{out} - \dot{E}x_{in}}{\dot{W}_{pump}}$	(14)	Exergy efficiency of pump
$\varepsilon_{system} = \frac{\dot{E}x_{useful,HE}}{\dot{E}x_{brine}} = 1 - \frac{\dot{E}x_{dest,system} + \dot{E}x_{reinjected} + \dot{E}x_{pipelinelosses}}{\dot{E}x_{brine}}$	(15)	System exergy efficiency

were calculated from Eqs. (4) and (6), respectively, namely using related name location (state) numbers (21–24, 32–36) in Fig. 1, corresponding to the thermal energy and exergy input to BGDHS.

It is usually more convenient to find entropy generation $\dot{S}_{gen}$ first and then evaluate the exergy destruction due to irreversibility $\dot{E}x_{dest}$ directly from Eqs. (7)–(10) given in Table 1.

Two types of pumps have been used in BGDHS: lineshaft pumps and centrifugal pumps. Lineshaft pumps are used to pump thermal water from geothermal reservoir to surface. Centrifugal pumps are used to transmit and circulate the thermal water and water in the pipeline systems. These pumps are controlled by a variable frequency drive for energy economy. Technical staff (especially district heating operators) communications are used for pressure and temperature distributions along pipeline and the pump operating points in this work. Besides, in BGDHS, variable frequency drivers used to control the speed of the pumps. Actual power consumption ($\dot{W}_{pump}$) of each pump is read the display of the variable frequency drivers, that is flowmeter at each pump outlet, precisely. These data are collected from operators and storage. Using these data are calculated for ($\dot{W}_{pump}$) and efficiency of each pump in the study.

The energy efficiency of the system can be defined as the ratio of total energy output to total energy input: Eq. (11). In a similar way, we define exergy efficiency as the ratio of total exergy output to total exergy input: Eq. (12). The exergy efficiency of a heat exchanger is determined by the increase in the exergy of the cold stream divided by the decrease in the exergy of the hot stream on a rate basis as Eq. (13).

4. Results and discussion

The temperature, pressure, and mass flow rate data for both thermal water and water are given in accordance with their state numbers as specified in Fig. 1. The exergy rates are calculated for each state as listed in Table 2. The data were obtained from the measured values in the system and they were converted into SI units; therefore, pressure values were determined precisely in Table 2. Note that here state 0 indicates the reference state for both thermal and water. Some investigators (e.g., [8,9]) also employed this type of selection in the exergy analysis of geothermal power plants. For thermal water, the thermodynamic properties of water are used since the effects of salts and non-condensable gases that may exist

Table 2
Exergy rates and other thermodynamic properties of the states as shown in Fig. 1

State no.	Fluid type	Temperature T (°C)	Pressure P (kPa)	Specific enthalphy h (kJ/kg)	Specific entropy s (kJ/kgK)	Mass flow rate $\dot{m}$ (kg/s)	Specific exergy ψ (kJ/kg)	Energy rate $\dot{E}$ (kW)	Exergy rate $\dot{E}x$ (kW)
0	W	11.4	101.32	48.51	0.1716	—	—	—	—
1	TW	105	222.11	439.95	1.3623	11.2	52.626	4384.13	589.41
2	TWR	55	117.05	230.02	0.7671	11.2	12.060	2032.91	135.08
3	W	80	148.67	334.71	1.0744	18.71	29.308	5354.80	548.36
4	W	50	113.65	209.13	0.703	18.71	9.410	3005.20	176.06
5	TW	105	222.11	439.95	1.3623	5.82	52.626	2278.18	306.29
6	TWR	80	148.67	334.71	1.0744	5.82	29.308	1665.68	170.57
7	W	55	117.05	230.02	0.7671	9.72	12.060	1764.28	117.23
8	W	50	113.65	209.13	0.703	9.72	9.410	1561.23	91.47
9	TW	90	171.42	376.7	1.1917	4.88	37.921	1601.57	185.05
10	TWR	57	118.62	238.38	0.7952	4.88	12.425	926.57	60.63
11	W	85	159.11	355.71	1.1334	5.37	33.520	1649.66	180.00
12	W	55	117.05	230.02	0.7671	5.37	12.060	974.71	64.76
13	TW	90	171.42	376.7	1.1917	5.42	37.921	1778.79	205.53
14	TWR	57	118.62	238.38	0.7952	5.42	12.425	1029.10	67.34
15	W	85	159.11	355.71	1.1334	5.97	33.520	1833.98	200.11
16	W	55	117.05	230.02	0.7671	5.97	12.060	1083.61	72.00
17	TW	75	139.86	313.74	1.0146	25.47	25.354	6755.41	645.78
18	TWR	60	121.23	250.93	0.8303	25.47	14.987	5155.64	381.72
19	W	70	132.47	292.78	0.954	19.12	21.638	4670.44	413.72
20	W	50	113.65	209.13	0.703	19.12	9.410	3071.05	179.92
21	TW	102.3	354.63	428.73	1.3321	34.55	50.000	13136.60	1727.49
21′[a]	TW	102	210.1	427.29	1.3287	34.55	49.527	13086.85	1711.16
22	TW	106.7	354.63	447.3	1.3813	25.42	54.570	10137.24	1387.17
22′[a]	TW	106.4	228.1	445.87	1.3779	25.42	54.107	10100.89	1375.41
23	TW	101.1	354.63	423.67	1.3186	8.51	48.781	3192.61	415.13
23′[a]	TW	100.8	205.57	422.22	1.3152	8.51	48.299	3180.27	411.02
24	TW	101.4	486.36	425.04	1.3219	25.27	49.212	9514.91	1243.59
24′[a]	TW	101.1	206.68	423.49	1.3186	25.27	48.601	9475.74	1228.15
25	TW	116.7	324.24	489.59	1.4913	78.49	65.559	34620.37	5145.75
26	TW	117	557.28	491.02	1.4945	78.49	66.079	34732.61	5186.53
27	TW	62	506.62	259.68	0.8553	78.49	16.623	16574.73	1304.75
28	W	89.4	689.01	374.67	1.1847	150.78	37.882	49178.40	5711.91
29	W	60.7	420.49	254.18	0.8391	144.85	15.733	29791.30	2278.91
30	W	61	790.33	255.74	0.8428	150.78	16.240	31246.14	2448.67
31	W	13.3	350	56.66	0.1995	5.93	0.211	48.33	1.25
31′[a]	W	13	200	55.27	0.1951	5.93	0.073	40.09	0.43
32	TW	133.9	404.53	562.72	1.6748	19.13	86.474	9836.84	1654.26
32′[a]	TW	133.6	401.87	561.44	1.6717	19.13	86.077	9812.35	1646.64
33	TW	130.1	455.96	546.62	1.6349	19.98	81.728	9952.24	1632.93
33′[a]	TW	129.8	369.85	545.21	1.6317	19.98	81.229	9924.07	1622.95
34	TW	136.5	506.63	573.96	1.702	41.82	89.975	21974.32	3762.74
34′[a]	TW	136.2	425.5	572.56	1.6989	41.82	89.457	21915.77	3741.08
35	TW	120.4	557.28	505.45	1.5313	21.73	70.037	9929.31	1521.91
35′[a]	TW	120.1	300.51	503.92	1.5281	21.73	69.418	9896.06	1508.45
36	TW	117.5	455.96	493.08	1.5	15.75	66.574	7001.98	1048.54
36′[a]	TW	117.2	282.89	491.6	1.4967	15.75	66.033	6978.67	1040.02
37	TW	90	171.42	376.73	1.1917	3.66	37.951	1201.29	138.90
38	TWR	57	118.62	238.38	0.7925	3.66	13.193	694.92	48.29
39	W	85	159.11	355.71	1.1334	4.02	33.520	1234.94	134.75
40	W	55	117.05	230.02	0.7671	4.02	12.060	729.67	48.48
41	TW	105	222.11	439.95	1.3623	51.95	52.626	20335.31	2733.94
42	TWR	65	126.32	271.85	0.8925	51.95	18.208	11602.51	945.90
43	W	80	148.67	334.72	1.0744	104.72	29.318	29971.91	3070.21
44	W	60	121.24	250.93	0.8303	104.72	14.987	21197.42	1569.43
45	TW	107.3	486.36	449.94	1.388	1.32	55.303	529.89	73.00
46	TWR	78.7	303.97	327.76	1.0541	1.32	28.135	368.61	37.14
47	W	80	162.12	334.78	1.0744	2.09	29.378	598.30	61.40
48	W	61.7	212.78	258.18	0.8515	2.09	16.204	438.21	33.87
49	TW	110	486.36	461.35	1.4179	0.2	58.205	82.57	11.64
50	TWR	50	113.65	209.13	0.703	0.2	9.410	32.12	1.88

Table 2 (*continued*)

State no.	Fluid type	Temperature T (°C)	Pressure P (kPa)	Specific enthalpy h (kJ/kg)	Specific entropy s (kJ/kgK)	Mass flow rate $\dot{m}$ (kg/s)	Specific exergy ψ (kJ/kg)	Energy rate $\dot{E}$ (kW)	Exergy rate $\dot{E}$x (kW)
51	W	65	263.44	272.02	0.8925	0.42	18.378	93.87	7.72
52	W	36.6	273.57	153.52	0.5264	0.42	4.052	44.10	1.70
53	TW	111.6	486.36	460.11	1.4355	9.4	51.957	3869.04	488.40
54	TWR	80	148.67	334.71	1.0744	9.4	29.308	2690.28	275.50
55	W	81	303.97	339.09	1.0863	12.83	30.302	3728.14	388.78
56	W	57.7	364.77	241.59	0.8014	12.83	13.870	2477.22	177.96
57	TW	108	425.56	452.85	1.3957	16.3	56.022	6590.74	913.16
58	W	90	496.49	377.04	1.1917	24.21	38.261	7953.71	926.29
59	W	56	385	234.51	0.7798	24.21	12.937	4503.06	313.20
60	W	56.3	618.08	235.96	0.7836	24.21	13.305	4538.16	322.12
61[b]	—	—	—	—	—	—	—	—	—
61′[b]	—	—	—	—	—	—	—	—	—
62	TWR	58	398.2	242.87	0.8051	16.3	14.098	3168.07	229.79
63	TW	58	398.2	242.87	0.8051	16.3	14.098	3168.07	229.79
63′[b]	TW	57.7	119.2	241.31	0.8013	16.3	13.619	3142.64	221.99
64	TWR	40	108.69	167.37	0.572	16.3	4.926	1937.42	80.30
65	W	47	111.93	196.6	0.6642	29.84	7.921	4419.01	236.35
66	W	37	107.6	154.85	0.5319	29.84	3.817	3173.19	113.89
67	TWR	64	364.77	267.93	0.8801	114.76	17.816	25180.64	2044.60

Note: The phase of the reference state is liquid.

[a]Calculated data.

[b]It was not operated on the particular day data were taken. (0): Reference state. W: Water. TW: Thermal water. TWR: Thermal water re-injection.

in the geothermal brine are neglected as observed by Kanoglu [8].

The exergy efficiencies and destructions for the entire system and its major system components are listed in Table 3.

Using Eqs. (1) and (2) in Table 1, the total geothermal reinjection fluid (as the thermal water reinjected into the well BD8) mass flow rate is 114.76 kg/s at an average temperature of 64 °C and the production well total mass flow rate is 212.16 kg/s, and the natural direct discharge of the system is then calculated to be 97.4 kg/s based on the data for 2nd January 2004.

This clearly indicates that in the BGDHS there is a significant amount of water lost through leaks and drippings in the water distribution network, which was made of carbon steel pipe and wrapped with polyurethane foam insulating material (e.g., glasswool) to provide a sealing and insulation. This was a result of poor operation, maintenance and control of the distribution network.

Using the values given in Table 3, Eqs. (11) and (12) in Table 1, the energy and exergy efficiencies of the BGDHS are determined to be 42.36% and 46.55%, respectively. The energy balance diagram for the system is illustrated in Fig. 2. The thermal reinjection accounts for 26.59% of the total energy input, while the pipeline losses of the system cover its 31.05%, and the heat exchangers gain 42.36%.

For analysis purposes the actual thermal data for energy and exergy analysis and performance assessment purposes were taken from the BGDHS on 2nd January 2004, and the respective thermodynamic properties were obtained based upon these data. It is important to note that the number of the operational wells in the Balcova geothermal field may vary depending on the heating days and operating strategy.

The exergy flow diagram is given in Fig. 3 and shows that 53.45% of the total exergy flow entering the system is lost, while the remaining 46.55% is utilized. The highest exergy loss is found to be 28.70% from the distribution pipeline of the system due to a significant amount of water leaks and includes some part of the exergy destructions through the primary and secondary fluid networks, which were not studied in this paper. The second largest exergy destruction occurs from the thermal reinjection as 14.18% of the total exergy input. This is followed by the total exergy destruction associated with the heat exchangers and pumps amounts to some 1.52 MW, which accounts for 10.57% of the total exergy input to the system.

In addition, Figs. 4 and 5 show the bar charts of energy and exergy rates; showing the total energy and inputs, energy and exergy losses due to the thermal reinjection, energy and exergy losses due to the water leaks and drips in the distribution network, exergy product, and exergy destructions in the pumps and heat exchangers. These calculated values were found using

Table 3
Some exergetic, energetic and thermodynamics analysis data provided for one unit of the system (reference state temperature and the atmospheric pressure are 11.4 °C and 101.32 kPa, respectively)

Item no. (k)	Component	Exergy destruction rate (kW) ($\dot{E}x_{dest}$) (ExHEL, ExPu, ExpLL, ExTR)	Utilized power (kW) ($\dot{E}_{useful}$)	Heat transfer rate or installed power (kW)	$\dot{P}$ (kW)	TEI (kW)	ETR (kW)	EPLL (kW)	TExI (kW)	ExTR (kW)	ExP (kW)	Exergy efficiency ε (%)	Energy efficiency η (%)
1	Heat exchanger: I	618.54	18157.09	50364	3263.23	—	—	—	—	—	3263.23	84	—
2	II	79.21	3422.18	5800	604.16	—	—	—	—	—	604.16	88	—
3	III	27.03	1226.99	2310	122.46	—	—	—	—	—	122.46	82	—
4	IV	82.04	2350.32	3372	372.29	—	—	—	—	—	372.29	82	—
5	V	109.95	1221.33	4651	25.76	—	—	—	—	—	25.76	19	—
6	VI	9.18	675.08	220	115.24	—	—	—	—	—	115.24	93	—
7	VII	10.08	749.78	1700	128.11	—	—	—	—	—	128.11	93	—
8	VIII	30.26	1600.02	3200	233.80	—	—	—	—	—	233.80	89	—
9	IX	4.35	506.31	1275	86.27	—	—	—	—	—	86.27	95	—
10	X	287.26	8729.68	15700	1500.78	—	—	—	—	—	1500.78	84	—
11	XI	8.33	161.71	2326	27.53	—	—	—	—	—	27.53	77	—
12	XII	3.74	50.36	1117	6.02	—	—	—	—	—	6.02	62	—
13	XIII	2.08	1251.43	1316	210.82	—	—	—	—	—	210.82	99	—
14	Well pump: B10	11.12	27.45	45	16.33	13136.60	—	—	1727.49	—	—	18.9–59	65–80
15	B5	26.49	38.25	75	11.76	10137.24	—	—	1387.17	—	—	8.8–31	65–80
16	B4	9.64	13.75	55	4.11	3192.61	—	—	415.13	—	—	9.6–30	65–80
17	B1	15.91	31.35	55	15.44	9514.91	—	—	1243.59	—	—	23.5–49	65–80
18	BD2	7.39	15	75	7.61	9836.84	—	—	1654.26	—	—	0.3–51	65–80
19	BD3	28.52	38.5	110	9.98	9952.24	—	—	1632.93	—	—	4.8–26	65–80
20	BD4	31.14	52.8	110	21.66	21974.32	—	—	3762.74	—	—	6.9–41	65–80
21	BD5	17.34	30.8	55	13.46	9929.31	—	—	1521.91	—	—	19.2–44	65–80
22	BD7	23.93	32.45	55	8.52	7001.98	—	—	1048.54	—	—	8.9–26	65–80
23	Reinjection well	—	—	—	—	—	25180.64	—	—	2044.60	—		
24	Balcova booster pump	27.23	68	200	40.77	—	—	—	—	—	—	28.4–60	65–80
25	Balcova circ. pump	22.23	192	480	169.77	—	—	—	—	—	—	28.4–88	65–80
26	Pressurized water tank (Balcova)	10.18	11	11	0.82	—	—	—	—	—	—	7–8	65–80
27	Narlidere circ. pump	6.07	15	30	8.93	—	—	—	—	—	—	0.60–38	65–80
28	Pressurized water tank (Narlidere)	0	—	4	0	—	—	—	—	—	—	—	65–80
29	Caglayan booster pump	14.20	22	22	7.80	—	—	—	—	—	—	21–35	65–80
30	Heat exchangers and pumps	1523.46	40690.63	96643	7033.42	—	—	—	—	—	—	—	—
31	Overall system	7697.26	7033.42	96643	7033.42	94676.05	25180.64	29390	14393.76	2044.60	6696.47	46.55	42.36

data set, on 2nd January 2004, and reference temperatures and atmospheric pressure were assumed as 0, 25 °C and 101.32 kPa, respectively. Furthermore, energy and exergy efficiency values are correlated and illustrated in Fig. 6 with a high correlation coefficient ($R^2 = 0.99$). As seen in the figure, energy and exergy efficiencies of the BGDHS vary between 38% and 49% and 45% and 47%, respectively. We also conduct an error/uncertainty analysis, using the method mentioned earlier [19] based on the actual data, to determine the uncertainties in the calculated values of energy and exergy efficiencies and tabulate in Table 3. Here, we note that variable speed pumps do not run efficiently enough.

The total energy input values are obtained for a range from 82.67 to 104.75 MW for different reference state values, basically from 0 to 25 °C for a better coverage and presentation of how the varying reference state temperature affects the performance of the system in terms of energy and exergy efficiencies. In conjunction with this, the total exergy input values are obtained to be from 10.92 to 17.67 MW for the same days. As expected, the lower the reference state temperature, the significantly larger the energy and exergy losses in the system pipeline and heat exchangers (Figs. 4 and 5). However, energy and exergy rates of pipeline losses of the system, heat exchangers, and useful exergy increase considerably. The reason for this rapid rise in energy and exergy rates is due to a decrease in the ambient temperature, as shown in Figs. 4 and 5. Based on these, we do curve-

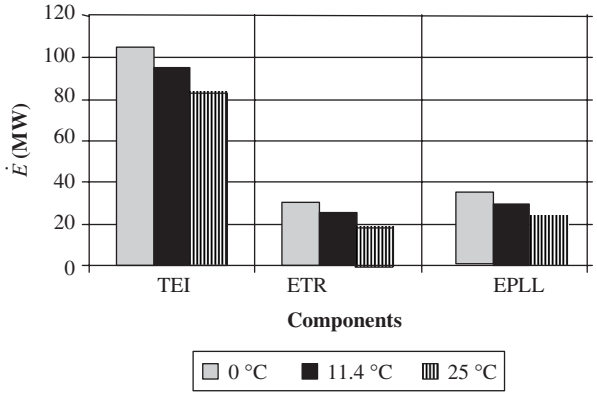

Fig. 4. Bar chart of energy rates for various system components at three different reference state temperatures (reference state temperature and the atmospheric pressure are 11.4 °C and 101.32 kPa, respectively).

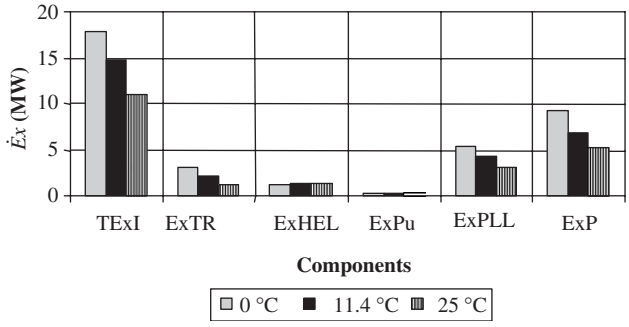

Fig. 5. Bar chart of exergy rates for various system components at three different reference state temperatures (reference state temperature and the atmospheric pressure are 11.4 °C and 101.32 kPa, respectively).

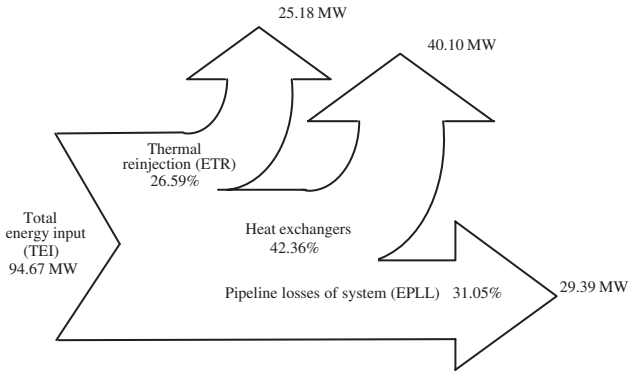

Fig. 2. System energy flow diagram (reference state temperature and the atmospheric pressure are 11.4 °C and 101.32 kPa, respectively).

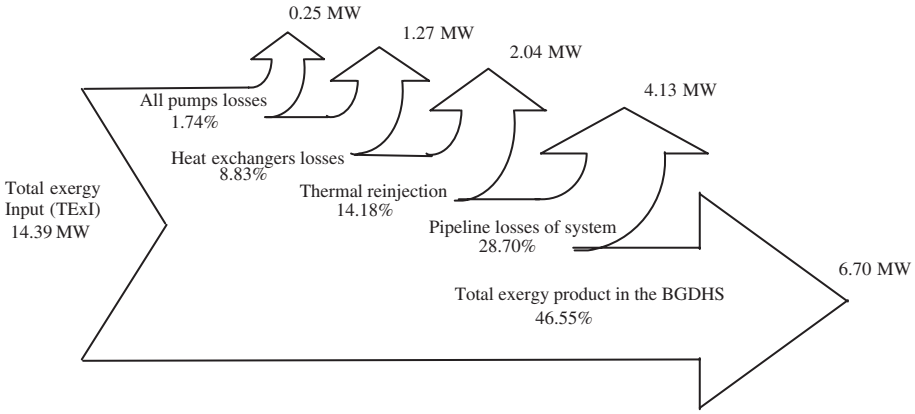

Fig. 3. System exergy flow diagram (reference state temperature and the atmospheric pressure are 11.4 °C and 101.32 kPa, respectively).

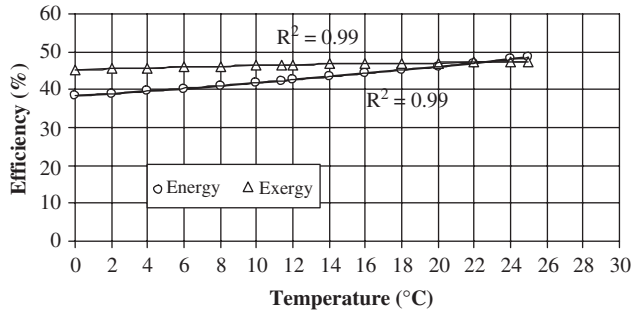

Fig. 6. Variation of energy and exergy efficiencies with the reference temperature.

fitting to observe the trend of the energy and exergy efficiencies of the BGDHS as follows:

- Energy efficiency correlation becomes:

$$\eta_{c1} = 2E-05T_a^3 - 0.0029T_a^2 + 0.3228T_a + 38.274, \quad (16)$$

- Exergy efficiency correlation becomes:

$$\varepsilon_{c2} = -6E-05T_a^3 + 0.004T_a^2 - 0.1279T_a + 45.21, \quad (17)$$

where T_a is ambient temperature (°C).

These correlations are capable of predicting the values of energy and exergy efficiencies of the BGDHS for different environment temperatures.

In conclusion, the results presented here suggest that exergy analysis appears to be a potential tool in determining locations, types and true magnitudes of wastes and losses, furthering the objective of more efficient energy resource utilization, and revealing whether or not and how much it is possible to design more efficient geothermal district heating systems by reducing the inefficiencies in the systems and their components.

5. Conclusions

We conduct an energy and exergy analysis of the geothermal district heating systems and apply to the BGDHS in Izmir, Turkey as a case study at a reference temperature of 11.4 °C. We also utilize actual thermal data taken from the system to perform a system performance assessment through energy and exergy efficiencies. Moreover, the exergy destructions (showing the losses) in the overall system are quantified and illustrated using an exergy flow diagram along with an energy flow diagram. Two empirical correlations are developed to estimate the effective energy and exergy efficiencies. We can draw some key concluding remarks as follows:

- The total energy input values range from 82.67 to 104.75 MW for the reference state temperatures from 0 to 25 °C while the total exergy input values vary from 10.92 to 17.67 MW, respectively.
- The energy and exergy efficiencies of the BGDHS vary between 38% and 49%, and 45% and 47% at the varying reference temperatures from 0 to 25 °C, respectively.
- BGDHS has a great amount of water leakages, resulting in large pipeline losses which reduces energy and hence exergy content.
- Although variable speed drive is used for the line shaft pumps and centrifugal pumps for efficient energy use, this shows no essential effect on the exergy efficiency.
- The district heating supply temperature should be selected as high as possible to increase the exergy efficiency of the heat exchangers and hence the whole system in consistent with the operating strategies.

Acknowledgements

The authors gratefully acknowledge the support provided for this work by the Izmir-Balcova Geothermal Inc. (IBGI) and personal support by its general manager, Mr. Fasih Kutluay.

References

[1] Mock JE, Tester JW, Wright PM. Geothermal energy from the earth: its potential as an environmentally sustainable resource. Annual Review of Energy and the Environment 1997;22:305–56.
[2] Wepfer WJ, Gaggioli RA. Reference datums for available energy. In: Gaggioli RA, editor. Thermodynamics: second law analysis. ACS symposium series 122. Washington, DC: American Chemical Society; 1980. p.77–92.
[3] Etele J, Rosen MA. Sensitivity of exergy efficiencies of aerospace engines to reference environment selection. Exergy—An International Journal 2001;1:91–9.
[4] Rosen MA, Dincer I. Effect of varying dead state properties on energy and exergy analyses of thermal systems. International Journal of Thermal Sciences 2004;43:121–33.
[5] Badvarsson G, Eggers DE. The exergy of thermal water. Geothermics 1972;1:93–5.
[6] Dipippo R, Marcille DF. Exergy analysis of geothermal power plants. Geothermal Resources Council Transactions 1984;8:47–52.
[7] Dipippo R. Second law analysis of flash-binary and multilevel binary geothermal plants. Geothermal Resources Council Transactions 1994;18:505–10.
[8] Kanoglu M. Exergy analysis of a dual-level binary geothermal power plant. Geothermics 2002;31:709–24.
[9] Cerci Y. Performance evalution of a single-flash geothermal power plant in Denizli, Turkey. Energy 2003;28:27–35.
[10] Brook CA, Mariner RH, Mabey DR, Swanson JR, Guffani M, Muffler LJP. Hydrothermal convection system with reservoir temperature ⩾90 °C. In: Muffler LJP, editor. Assessment of

geothermal resources of the United States—1978. US Geological Survey Circular 790, Library of Congress Card No. 79-600006, 1979. p. 18–85.
[11] Quijano J. Exergy analysis for the Ahuachapan and Berlin Geothermal fields, El Salvador. Proceedings world geothermal congress, May 28–June 10 2000, Kyushu-Tohoku, Japan.
[12] Lee KC. Classification of geothermal resources by exergy. Geothermics 2001;30:431–42.
[13] Rosen MA, Dincer I. A study of industrial steam process heating through exergy analysis. International Journal of Energy Research 2004;28(10):917–30.
[14] Ozgener L, Hepbasli A, Dincer I. Thermo-mechanical exergy analysis of Balcova geothermal district heating system in Izmir, Turkey. ASME-Journal of Energy Resources Technology 2004;126(4):293–301.
[15] Ozgener L, Hepbasli A, Dincer I. Energy and exergy analysis of Salihli geothermal district heating system in Manisa, Turkey. Inernational Journal of Energy Research 2005;29:393–408.
[16] Ozgener L, Hepbasli A, Dincer I. Energy and exergy analysis of geothermal district heating systems: an application. Building and Environment, in press; 2005.
[17] Ozgener L. Exergoeconomic analysis of geothermal district heating systems. Ph.D. Thesis, Natural and Applied Sciences, Mechanical Engineering Science Branch, Ege University, 2005, pp. 102 (in Turkish).
[18] Harrison R, Mortimer ND, Smarason OB. In: Geothermal heating: a handbook of engineering economics. New York: Pergamon Press; 1990. p. 558.
[19] Holman JP. Experimental methods for engineers, 7th ed. New York: McGraw-Hill; 2001. p. 48–143.